Preamble Detection Based on Cyclic Features of Zadoff–Chu Sequences for Underwater Acoustic Communications

Qingyuan Tan , Yiyin Wang , *Member, IEEE*, and Xiaoli Ma, *Fellow, IEEE*

Abstract—**Preamble detection is an important yet challenging task for underwater acoustic communications. The received preamble is distorted by unknown multipath propagation, severe Doppler scaling effect, various noise, and external interference in underwater scenarios. In this letter, we propose a cyclic feature detector using a Zadoff–Chu sequence by exploiting its cyclic features. The Doppler scale information is carried by these cyclic features. The proposed detector can bypass the requirement of channel information and is robust to carrier frequency offset. Moreover, it can deal with noise uncertainty and impulsive interference. Simulation and experimental results show that the proposed detector significantly outperforms the state of the art in detection performance.**

Index Terms—**ZC sequence, Doppler scale, cyclic feature detector, underwater acoustic communications.**

I. INTRODUCTION

UNDERWATER acoustic communications (UAC) are key enabling technologies for underwater exploration, offshore defense, environment monitoring, etc. Preamble detection is usually the first task to be accomplished in an UAC receiver and thus very important. Via an underwater acoustic channel, a preamble signal is greatly impacted by the Doppler scaling effect and the multipath propagation [1]. Moreover, it is corrupted by various ambient noise and interference. Due to the lack of prior information about channel, noise, and interference, the preamble detection is in general challenging.

The conventional preamble signals are Doppler-insensitive waveforms, such as linear frequency modulation (LFM) and hyperbolic frequency modulation (HFM) signals. They can be tolerant on the Doppler scaling effect in a limited range. Hence, the matched filter (MF) and normalized matched filter (NMF) types of detectors are employed to correlate the received signal with a local template for detection [2, Chap. 6]–[4]. However, due to the multipath effect, the detection performance degrades as only the strongest path is utilized in these detectors. Furthermore, the sign correlation (SC) detector [5] is proposed to deal with the impulsive interference, which is frequently encountered in underwater environments. The SC detector still does not consider the channel impact. More recently, energy concentration (EC) and accumulated correlation coefficients (ACC) detectors are proposed in [6]. They make use of the sparse signal reconstruction and show more robust performance than the existing MF based detectors. The LFM preamble is employed in [6]. Therefore, the Doppler scaling effect is ignored. Apart from the Doppler-insensitive preambles, Doppler-sensitive waveforms can be used as preambles as well. Due to the Doppler scaling effect, the detection is coupled with the Doppler scale estimation. A preamble composed of two consecutive identical orthogonal frequency division multiplexing (OFDM) symbols is proposed in [7]. Accordingly, normalized cross-correlation based 2D-search method is developed to detect the signal and estimate the Doppler scale jointly.

Different from conventional preambles, we are interested in applying Zadoff-Chu (ZC) sequences as preambles for underwater communications. The reason is two-fold: i) the ZC sequences are constant-amplitude zero autocorrelation (CAZAC) sequences, which have excellent autocorrelation and cross-correlation properties. They are employed for synchronization in the Long Term Evolution (LTE) standard [8]; ii) the ZC sequences are double-sided to the Doppler-sensitivity. It is Doppler insensitive when its root index parameter is small. Actually, the ZC sequence can be regarded as the digital implementation of the LFM signal with the same length, when its root index is one. On the contrary, the ZC sequence is Doppler sensitive when its root index parameter is large. Hence, we have more design freedom about the ZC sequences. In [9], a preamble is designed to be consisted of two consecutive identical ZC sequences. A detector similar to the one in [7] is used. In [10], a generalized likelihood ratio test (GLRT) detector is proposed to use ZC sequences taking the multipath effect and carrier frequency offset (CFO) into account.

In this letter, we propose a preamble detection method using a ZC sequence, and consider the Doppler scaling effect and the multipath propagation with ambient noise and impulsive interference. Accordingly, we investigate the cyclic features of the ZC sequence and propose a cyclic feature detector (CFD). The CFD is well known for its robustness to noise uncertainty and strong interference [11], [12, Chap. 17], [13]. Thus, it is suitable to deal with underwater scenarios. Furthermore, the proposed CFD does not need the multipath channel information. The cyclic features collect the multipath energy and carry the information about the

Doppler scale. In addition, the CFD is robust to the CFO impact. By simulations and using channel measurements, we verify that the proposed CFD outperforms the existing popular detectors.

II. System Model

In this section, we introduce the models for the transmitted preamble signal, the underwater acoustic channel, the composite noise and the received signal, respectively.

A. The Transmitted Signal

Due to the good properties of the ZC sequence, we use it as a preamble. To facilitate the implementation, a ZC sequence with an even length is chosen as

$$s[n] = e^{j\frac{\pi}{N}un^2}, 0 \leq n \leq N-1, \tag{1}$$

where the length of the sequence N is an even number, and the root index u is an integer relatively prime to N. Since the Doppler scaling effect of the underwater channel squeezes or stretches the transmitted signal, the preamble sequence is written in a continuous form to analyze the Doppler scaling effect. As the sampling period of the baseband signal is assumed as T_s, the continuous baseband waveform of the transmitted signal can be written as

$$s(t) = \sum_{n=0}^{N-1} s[n]\rho(t - nT_s), 0 \leq t \leq NT_s, \tag{2}$$

where $\rho(t)$ is a pulse shaper, and its bandwidth is B ($B \approx 1/T_s$). The corresponding passband signal can be described as $\tilde{s}(t) = \sqrt{2}\mathcal{R}e\{e^{j2\pi f_c t}s(t)\}$, where f_c is the carrier frequency of the transmitter.

B. The Underwater Acoustic Channel Model

The transmitted passband signal goes through a time-varying multipath channel, which is modeled as a single-scale multi-lag (SSML) channel [2, Chap. 6] and given by

$$h(t, \tau) = \sum_{p=0}^{P-1} A_p \delta(\tau - \tau_p + \gamma t), \tag{3}$$

where P is the total number of paths, γ is the common Doppler scale for all paths, A_p is the channel gain of the pth path, and τ_p is the propagation delay of the pth path. We assume that all the paths share the same Doppler scaling factor γ and the path gains do not change during the transmission. Furthermore, the paths are independent with each other.

C. The Composite Noise Model

The underwater environment has various kinds of noise. The ambient noise comes from a wide range of sources [14, Chap. 4]. Furthermore, due to human and biological activities, the impulsive interference is frequently encountered [5], [15], such as snapping shrimp noise. It is characterized by high amplitude but very short duration. For the convenience of derivation, we employ a two-component Gaussian mixture (GM) model [16] for noise modeling. It is given by

$$u[n] = w[n] + i[n], \tag{4}$$

where $w[n]$ and $i[n]$ are the ambient noise and impulsive interference, respectively. The probability density function (PDF) of this model is $f(u[n]) = (1-g)\mathcal{CN}(u[n]; 0, \sigma_w^2) + g\mathcal{CN}(u[n]; 0, \sigma_w^2 + \sigma_i^2)$, where $\mathcal{CN}(\cdot)$ is a complex Gaussian distribution function, σ_w^2 is the variance of the additive white Gaussian noise (AWGN), σ_i^2 is the variance of the Gaussian component of the impulsive interference, and g is the probability of the occurrence of the impulsive interference. Note that the composite noise can be modeled by the symmetric α-stable (SαS) distribution according to [5] as well. However, it is difficult for derivation. Thus, we only test the SαS distributed noise in the simulation.

D. The Received Signal

Accordingly, the received passband signal can be written as

$$\tilde{r}(t) = \tilde{s}(t) \otimes h(t, \tau) + \tilde{u}(t)$$
$$= \sqrt{2}\mathcal{R}e\left\{e^{j2\pi(1+\gamma)f_c t}\sum_{p=0}^{P-1}\tilde{A}_p s((1+\gamma)t-\tau_p)\right\} + \tilde{u}(t), \tag{5}$$

where $\otimes$ represents the convolution, $\tilde{u}(t)$ represents the passband composite noise, and $\tilde{A}_p = A_p e^{-j2\pi f_c \tau_p}$. The received passband signal $\tilde{r}(t)$ is first downshifted to the baseband signal as $r(t) = \text{LPF}\{\tilde{r}(t)e^{-j2\pi \tilde{f}_c t}\}$, where $\tilde{f}_c$ is the carrier frequency of the receiver and $\text{LPF}\{\cdot\}$ is a low-pass filter. As a result, we arrive at

$$r(t) = e^{j2\pi f_o t}\sum_{p=0}^{P-1}\tilde{A}_p s((1+\gamma)t - \tau_p) + u(t), \tag{6}$$

where the CFO $f_o = f_c - \tilde{f}_c + \gamma f_c$, and $u(t)$ represents the equivalent baseband composite noise. Sequentially, the baseband signal is oversampled by a sampling period of T_r, where $T_r/T_s = 1/\lambda$ with an integer λ as the oversampling ratio. Thus, the received samples are

$$r[m] = e^{j2\pi f_o mT_r}\sum_{p=0}^{P-1}\tilde{A}_p s((1+\gamma)m/\lambda - d_p) + \acute{u}[m], \tag{7}$$

where $d_p = \tau_p/T_s$, and $\acute{u}[m]$ is the oversampling result of $u(t)$.

III. The Proposed Detection Method

In this section, we first show that the autocorrelation of the ZC sequence corrupted by the composite noise is periodical. Hence, its cyclic features can be extracted. In the same way, the received signal $r[m]$ manifests similar cyclic features, which carry the information of the Doppler scale. As a result, we calculate the cyclic autocorrelation functions (CAFs) of $r[m]$ and propose a detector based on the cyclic features.

Let us first investigate the cyclic features of the ZC sequence corrupted by the composite noise. Define $x[n] = s[n] + u[n]$. The autocorrelation $c_{x^*x}[n; l]$ of $x[n]$ is given by

$$c_{x^*x}[n; l] = E\{x^*[n]x[n + l]\}$$
$$= e^{j2\pi\frac{ul}{N}n+j\frac{\pi}{N}ul^2} + \sigma_w^2\delta(l) + g\sigma_i^2\delta(l), \tag{8}$$

which exhibits almost periodicity with respect to n. Its CAF is defined as $C_{x^*x}[f; l] = \lim_{N\to\infty}\frac{1}{N}\sum_{n=0}^{N-1}c_{x^*x}[n; l]e^{-j2\pi fn}$,

and given by

$$C_{x^*x}[f; l] = e^{j\frac{\pi}{N}ul^2}\delta(f - \frac{ul}{N}) + (\sigma_w^2\delta(l) + g\sigma_i^2\delta(l))\delta(f), \tag{9}$$

where $f = ul/N$ being the cyclic frequency (CF). We observe that when there is only the composite noise, $C_{x^*x}[f; l]$ is only nonzero at $f = 0$. On the other hand, $C_{x^*x}[f; l]$ is also nonzero at $f = ul/N$ when the ZC sequence appears. Hence, we can test $C_{x^*x}[f; l]$ at $f = ul/N$ to decide the appearance of the ZC sequence.

Moreover, the ZC sequence goes through an SSML channel, and then is downconverted and oversampled by a ratio λ. Due to the Doppler scale and the oversampling, the cyclic features of the received signal $r[m]$ change [13]. Then we investigate the autocorrelation $c_{r^*r}[m; \lambda]$ of $r[m]$. Because of the Doppler scale, an exact single shift for the received sequence is that $(1 + \gamma)T_s = (1 + \gamma)\lambda T_r$. In order to reduce the mismatch of the received sequences due to the unknown γ and $\gamma\lambda T_r \approx 0$, we use the single shift and set the delay lag $l = \lambda$. As a result, the autocorrelation $c_{r^*r}[m; \lambda]$ is given by

$$c_{r^*r}[m; \lambda] \approx Me^{j2\pi\frac{u(1+\gamma)^2}{\lambda N}m} + c_{w^*w}(\lambda) + c_{i^*i}(\lambda), \tag{10}$$

where M is an aggregate channel parameter taking the multipath and the CFO into account, $c_{w^*w}(\lambda)$ and $c_{i^*i}(\lambda)$ are time-invariant constants about the ambient noise the impulsive interference, respectively. More detailed derivations about the autocorrelation can be found in Appendix. Accordingly, the CAF $C_{r^*r}[f; \lambda]$ can be derived and is nonzero at the CF $u(1 + \gamma)^2/(\lambda N)$ when the preamble is present. Note that the CFO does not have any impact on the cyclic features, but the Doppler scale and the oversampling ratio influence.

As we do not know the exact value but a range of the Doppler scale γ, we choose several candidate CFs for detection based on the prior information as $f_i = f_{\min} + (i - 1)\Delta f$ and $f_i \in F$, where $F = \{f_{\min}, f_{\min} + \Delta f, \ldots, f_{\max}\}$, Δf is the step size for search. The cardinality of F is N_f. Sequentially, let us define the observation window length $N_s = \lambda N$. The CAF with the candidate CFs can be estimated as

$$\hat{C}_{r^*r}[f_i; \lambda] = \frac{1}{N_s}\sum_{m=0}^{N_s-1} r^*[m]r[m + \lambda]e^{-j2\pi f_i m}, f_i \in F. \tag{11}$$

The estimated CAFs are collected in row vectors as $\hat{\mathbf{z}}_i = [\mathcal{R}e(\hat{C}_{r^*r}[f_i; \lambda]), \mathcal{I}m(\hat{C}_{r^*r}[f_i; \lambda])], i = 1, \ldots, N_f$. In order to detect the presence of the cyclic features of the signal, two hypotheses are given by

$$\begin{aligned}\mathcal{H}_0 : \hat{\mathbf{z}}_i &= \xi_i, &&\text{preamble signal is absent,}\\ \mathcal{H}_1 : \hat{\mathbf{z}}_i &= \mathbf{z}_i + \xi_i, &&\text{preamble signal is present,}\end{aligned} \tag{12}$$

where $\mathbf{z}_i$ is the true CAF and ξ_i is the estimation errors. The error vector ξ_i is usually assumed to be asymptotically Gaussian distributed [17] as $\xi_i \sim \mathcal{N}(0, \Sigma_i)$, where Σ_i is a 2×2 asymptotic covariance matrix of $\hat{\mathbf{z}}_i$. The asymptotic covariance matrix Σ_i can be computed as

$$\Sigma_i = \begin{bmatrix} \mathcal{R}e\left(\frac{Q_i + P_i}{2}\right) & \mathcal{I}m\left(\frac{Q_i - P_i}{2}\right) \\ \mathcal{I}m\left(\frac{Q_i + P_i}{2}\right) & \mathcal{R}e\left(\frac{P_i - Q_i}{2}\right) \end{bmatrix}, \tag{13}$$

where Q_i and P_i are defined as $Q_i = S_{\lambda,\lambda}(2f_i, f_i)$, and $P_i = S_{\lambda,\lambda}(0, -f_i)$, respectively [17], with $S_{l_i,l_j}(f_i, f_j)$ being the cyclic spectrum of $c_{r^*r}[m; \lambda]$. The estimate of $S_{l_i,l_j}(f_i, f_j)$

can be obtained by the frequency smoothed cyclic periodograms (see (23) in [17]).

According to the test hypotheses and the asymptotic normality of $\hat{\mathbf{z}}_i$, the generalized likelihood ratio test (GLRT) [18] decides $\mathcal{H}_1$ if

$$\frac{p(\hat{\mathbf{z}}_i; \overline{\mathbf{z}}_i, \hat{\Sigma}_i, \mathcal{H}_1)}{p(\hat{\mathbf{z}}_i; \hat{\Sigma}_i, \mathcal{H}_0)} = \frac{\exp\left(-\frac{1}{2}N_s(\hat{\mathbf{z}}_i - \overline{\mathbf{z}}_i)\hat{\Sigma}_i^{-1}(\hat{\mathbf{z}}_i - \overline{\mathbf{z}}_i)^T\right)}{\exp\left(-\frac{1}{2}N_s\hat{\mathbf{z}}_i\hat{\Sigma}_i^{-1}\hat{\mathbf{z}}_i^T\right)}$$

$$= \exp\left(\frac{1}{2}N_s\hat{\mathbf{z}}_i\hat{\Sigma}_i^{-1}\hat{\mathbf{z}}_i^T\right) > \Gamma_F, \tag{14}$$

where $p(\hat{\mathbf{z}}_i; \overline{\mathbf{z}}_i, \hat{\Sigma}_i, \mathcal{H}_1)$ is the PDF of the observation $\hat{\mathbf{z}}_i$ with the maximum likelihood estimate (MLE) of the mean $\overline{\mathbf{z}}_i$ and the covariance matrix $\hat{\Sigma}_i$ under $\mathcal{H}_1$, and $p(\hat{\mathbf{z}}_i; \hat{\Sigma}_i, \mathcal{H}_0)$ is the PDF of the observation $\hat{\mathbf{z}}_i$ with the MLE of the covariance matrix $\hat{\Sigma}_i$ under $\mathcal{H}_0$. Moreover, Γ_F is the threshold. Taking the logarithm of the generalized likelihood ratio and multiplying the result by 2, the test statistic $\mathcal{T}_i$ is obtained as

$$\mathcal{T}_i = N_s\hat{\mathbf{z}}_i\hat{\Sigma}_i^{-1}\hat{\mathbf{z}}_i^T. \tag{15}$$

Under the null hypothesis $\mathcal{H}_0$, we can approximately assume $\mathcal{T}_i \sim \chi_2^2$ for large N_s, where χ_2^2 is the central chi-squared distribution with 2 degrees of freedom. Under the alternative hypothesis $\mathcal{H}_1$, we arrive at $\mathcal{T}_i \sim \chi_2^2(N_s\mathbf{z}_i\Sigma_i^{-1}\mathbf{z}_i^T)$, where $\chi_2^2(\cdot)$ is the noncentral chi-squared distribution with 2 degrees of freedom.

As we have a set of candidate CFs (F), we propose to make use of the maximum of the test statistics over the candidate CF set to claim a detection if

$$\mathcal{D} \triangleq \max_i(\mathcal{T}_i) > \Gamma, i = 1, \ldots, N_f, \tag{16}$$

where the threshold Γ can be decided by a constant false alarm rate P_{fa} with $P_{\text{fa}} = P(\mathcal{D} \geq \Gamma \mid \mathcal{H}_0)$. Under the null hypothesis $\mathcal{H}_0$, the cumulative distribution function (cdf) of $\mathcal{D}$ can be computed as

$$P(\mathcal{D} \leq \Gamma) = P(\mathcal{T}_1 \leq \Gamma, \ldots, \mathcal{T}_{N_f} \leq \Gamma) = (1 - e^{-\frac{\Gamma}{2}})^{N_f}. \tag{17}$$

Hence, the threshold Γ is found to fulfill the condition that $P(\mathcal{D} \leq \Gamma) = 1 - P_{\text{fa}}$.

Furthermore, the following remarks are in order.

Remark 1. (Multi-scale effect): When the multipath components do not share the same Doppler scale factor, the performance of the proposed CFD will degrade. However, the CFD can still work as long as there is a dominant CF.

Remark 2. (Other common interference): The proposed CFD can accommodate other common interference [6], such as narrowband and similar sequence interference. As it rarely happens that these interference signals have the same cyclic features as the designed preamble. Hence, we can distinguish the preamble from the interference using cyclic features.

IV. PERFORMANCE WITH SIMULATIONS

In this section, the proposed detection method is evaluated and compared with other detection methods including MF, NMF, SC [5], EC and ACC [6] detectors. The PN sequence is used for the SC detector, and the LFM signal is used for all the other counterpart detectors. For a fair comparison, the parameters of the PN sequence and LFM are designed to be consistent with the ZC sequence. They are all through the same underwater acoustic

TABLE I
THE PREAMBLE PARAMETERS IN SIMULATIONS

System Parameters	Notation	Value
Preamble duration	NT_s	200 ms
Carrier frequency	f_c	13 kHz
Bandwidth	B	4.88 kHz
Length of the ZC sequence	N	976
Root index of the ZC sequence	u	11
Oversampling ratio	λ	10

Fig. 2. P_d vs. SNR at $P_{fa} = 10^{-3}$ with the GM modeled composite noise.
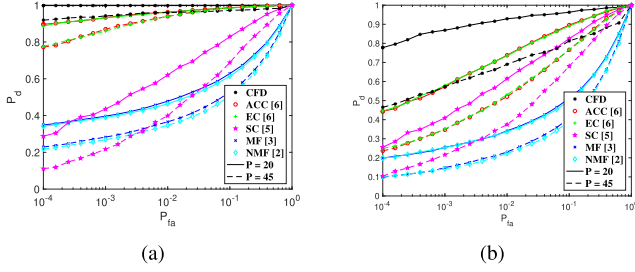
Fig. 1. ROC at SNR $= -14$ dB (a) with AWGN only and (b) with the GM modeled composite noise.

Fig. 3. ROC using WATERMARK with the SαS distributed composite noise.

channel. Table I shows the parameters of the ZC sequence used in the simulations. Furthermore, the SSML channel is generated according to [2, Chap. 6]. The amplitudes of paths follow a Rayleigh distribution with the average power decreasing exponentially with the delay. The power difference between the first path and the last one is 20 dB. The interarrival times of paths are assumed to follow an exponential distribution with a mean of 1ms. The Doppler scale is assumed to follow a uniform distribution within $[-3000, 3000]$ ppm. Using the GM noise model, the SNR is defined as SNR $= P_s/\sigma_w^2$, where P_s denotes the average power of the preamble symbols, and σ_w^2 denotes the variance of the ambient noise. The variance of the impulsive noise σ_i^2 is set to fulfill that $\sigma_i^2/\sigma_w^2 = 13$ dB and the probability of the occurrence of the impulsive noise $g = 0.01$.

We first compare the performance of different detectors using the SSML channel model. Fig. 1 shows the simulated receiver operating characteristic (ROC) curves [19, Chap. 4] at SNR $= -14$ dB with only AWGN and with the GM modeled composite noise, respectively. In both cases, MF and NMF have the worst performance. The EC and ACC detectors have moderate performance and their performance are very similar. The SC detector is worse than the EC and ACC detectors, but better than MF and NMF. Meanwhile the CFD achieves the best performance, as it takes advantage of the cyclic features of the ZC sequence and aggregates the multipath channel energy. Although the channel has the multipath effect, MF and NMF only use the strongest path, which degrades their performance. The SC detector has a similar problem, although it is still better than MF and NMF. For the ACC and EC detectors, they exploit multipath but the Doppler scaling effect is ignored. Hence, they are not as good as the CFD. As the number of paths increases, the performance of all detectors degrade. Sequentially, Fig. 2 shows P_d versus (vs.) SNR at $P_{fa} = 10^{-3}$ with the GM modeled composite noise. The overall trend is the same as the one in Fig. 1. Affected by the impulsive noise, the performance of all detectors is degraded. Nevertheless, the CFD still outperforms other detectors.

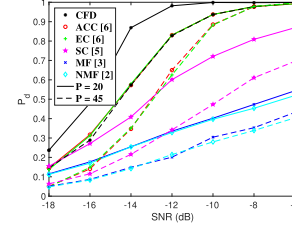Furthermore, we use the underwater acoustic channel replay benchmark (WATERMARK) [20] to test the detectors (the CFD
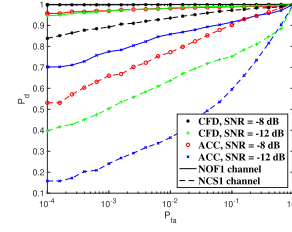
and ACC detectors, the best two according to Figs. 1 and 2) under realistic and reproducible conditions. We employ the NOF1 and NCS1 channel measurements. In general, NOF1 is a benign channel while NCS1 is a challenging one. The composite noise is modeled by the SαS distribution with $\alpha = 1.91$ as suggested in [5]. Thus, the SNR is defined as the ratio between signal power and noise dispersion as in [5]. Fig. 3 shows that the proposed CFD is better than the ACC detector in both channels. The detectors work better in NOF1 than in NCS1. The observations are consistent with those based on the simulations using the SSML channel and GM noise models.

APPENDIX

The autocorrelation $c_{r^*r}[m; \lambda]$ of $r[m]$ can be computed as

$$c_{r^*r}[m; \lambda] = E\{r^*[m]r[m + \lambda]\} \tag{18}$$

$$\approx e^{j2\pi f_o \lambda T_r} \sum_{p=0}^{P-1} E\{\tilde{A}_p^* \tilde{A}_p\} e^{j\frac{\pi}{N}u[(1+\gamma)^2 - 2(1+\gamma)d_p]} e^{j2\pi \frac{u(1+\gamma)^2}{\lambda N}m}$$

$$+ e^{j2\pi f_o \lambda T_r} \sum_{p,q,p \neq q}^{P-1} \left(E\{\tilde{A}_p^* \tilde{A}_q\} e^{j\frac{\pi}{N}u[(1+\gamma)^2 + d_q^2 - d_p^2 - 2(1+\gamma)d_q]} \right.$$

$$\left. e^{j2\pi \frac{u(1+\gamma)(1+\gamma+d_p-d_q)}{\lambda N}m} \right) + c_{w^*w}(\lambda) + c_{i^*i}(\lambda). \tag{19}$$

The first term in (19) is due to the autocorrelation of each path and the second is caused by the cross-correlation between different paths. Since the first term collects all the multipath energy at the CF $u(1+\gamma)^2/(\lambda N)$, it dominates in $c_{r^*r}[m; \lambda]$. The impact of the second term can be ignored. Let us define $M = e^{j2\pi f_o \lambda T_r} \sum_{p=0}^{P-1} E\{\tilde{A}_p^* \tilde{A}_p\} e^{j\frac{\pi}{N}u[(1+\gamma)^2 - 2(1+\gamma)d_p]}$. We arrive at

$$c_{r^*r}[m; \lambda] \approx M e^{j2\pi \frac{u(1+\gamma)^2}{\lambda N}m} + c_{w^*w}(\lambda) + c_{i^*i}(\lambda), \tag{20}$$

where the approximation is due to the omission of the second term.

REFERENCES

[1] P. Walree and R. Otnes, "Ultrawideband underwater acoustic communication channels," *IEEE J. Ocean. Eng.*, vol. 38, no. 4, pp. 678–688, Oct. 2013.

[2] S. Zhou and Z. Wang, *OFDM for Underwater Acoustic Communications*. John Wiley and Sons, Ltd., 2014.

[3] E. J. Kelly and R. P. Wishner, "Matched-filter theory for high-velocity, accelerating targets," *IEEE Trans. Mil. Electron.*, vol. 9, no. 1, pp. 56–69, Jan. 1965.

[4] R. Diamant, "Closed form analysis of the normalized matched filter with a test case for detection of underwater acoustic signals," *IEEE Access*, vol. 4, pp. 8225–8235, Nov. 2016.

[5] M. Chitre, J. Potter, and S. Ong, "Optimal and near-optimal signal detection in snapping shrimp dominated ambient noise," *IEEE J. Ocean. Eng.*, vol. 31, no. 2, pp. 497–503, Apr. 2006.

[6] W. Li, S. Zhou, P. Willett, and Q. Zhang, "Preamble detection for underwater acoustic communications based on sparse channel identification," *IEEE J. Ocean. Eng.*, vol. 44, no. 1, pp. 256–268, Jan. 2019.

[7] S. F. Mason, C. R. Berger, S. Zhou, and P. Willett, "Detection, synchronization, and Doppler scale estimation with multicarrier waveforms in underwater acoustic communication," *IEEE J. Sel. Areas Commun.*, vol. 26, no. 9, pp. 1638–1649, Dec. 2008.

[8] S. Sesia, I. Toufik, and M. Baker, *LTE—The UMTS Long Term Evolution: From Theory to Practice*, 2nd ed. Hoboken, NJ, USA: Wiley, Aug. 2011.

[9] Y. Li, Y. Wang, and X. Guan, "Joint synchronization and Doppler scale estimation using Zadoff-Chu sequences for underwater acoustic communications," in *Proc. IEEE OCEANS*, Anchorage, AK, USA, Sep. 2017, pp. 1–5.

[10] J. Tao and L. Yang, "Improved Zadoff-Chu sequence detection in the presence of unknown multipath and carrier frequency offset," *IEEE Commun. Lett.*, vol. 22, no. 5, pp. 922–925, Mar. 2018.

[11] S. Shamsunder and G. B. Giannakis, "Detection and estimation of chirp signals in non-Gaussian noise," in *Proc. IEEE Asilomar Conf. Signals, Syst. Comput.*, Pacific Grove, CA, USA, Nov. 1993, vol. 2, pp. 1191–1195.

[12] G. B. Giannakis, *Cyclostationary Signal Analysis*. Boca Raton, FL, USA: CRC Press, 1999.

[13] Z. Tian, Y. Tafesse, and B. M. Sadler, "Cyclic feature detection with sub-Nyquist sampling for wideband spectrum sensing," *IEEE J. Sel. Topics Signal Process.*, vol. 6, no. 1, pp. 58–69, Feb. 2012.

[14] X. Lurton, *An Introduction to Underwater Acoustics: Principles and Applications*, 2nd ed. Berlin, Germany: Springer-Verlag, 2010.

[15] J. A. Hildebrand, "Anthropogenic and natural sources of ambient noise in the ocean," *Mar. Ecol. Prog. Ser.*, vol. 395, no. 5, pp. 1–16, Dec. 2009.

[16] X. Kuai, H. Sun, S. Zhou, and E. Chen, "Impulsive noise mitigation in underwater acoustic OFDM systems," *IEEE Trans. Veh. Technol.*, vol. 65, no. 10, pp. 8190–8202, Oct. 2016.

[17] A. V. Dandawaté and G. B. Giannakis, "Statistical tests for presence of cyclostationarity," *IEEE Trans. Signal Process.*, vol. 42, no. 9, pp. 2355–2369, Sep. 1994.

[18] J. Lundén, V. Koivunen, A. Huttunen, and H. V. Poor, "Collaborative cyclostationary spectrum sensing for cognitive radio systems," *IEEE Trans. Signal Process.*, vol. 57, no. 11, pp. 4182–4195, Dec. 2009.

[19] S. M. Kay, *Fundamentals of Statistical Signal Processing, Volume II: Detection Theory*. Englewood Cliffs, NJ, USA: Prentice-Hall, 1998.

[20] P. Van Walree, F.-X. Socheleau, R. Otnes, and T. Jenserud, "The watermark benchmark for underwater acoustic modulation schemes," *IEEE J. Ocean. Eng.*, vol. 42, no. 4, pp. 1007–1018, May 2017.